Effect of pH on the Mechanism of Actin Polymerization†

Chris T. Zimmerle‡ and Carl Frieden*
Department of Biological Chemistry, Washington University School of Medicine, St. Louis, Missouri 63110
Received March 23, 1988; Revised Manuscript Received June 14, 1988

ABSTRACT: The effect of pH on the Mg^{2+}-induced polymerization of rabbit skeletal muscle G-actin at 20 °C was examined. Polymerization data were obtained at various initial concentrations of Mg^{2+}, Ca^{2+}, and G-actin between pH 6 and 7.5. The data were found to fit a kinetic mechanism for actin polymerization previously proposed at pH 8 in which Mg^{2+} binding at a moderate-affinity site on actin induces an isomerization of the protein enabling more favorable nucleation [Frieden, C. (1982) *J. Biol. Chem. 257*, 2882–2886]. The data also suggest the formation of actin dimers induced by Mg^{2+} binding is over 2 orders of magnitude more favorable at pH 6 than at pH 8. Little effect on trimer formation is found over this pH range. In addition, the conformation induced by nonspecific binding of metal to low-affinity sites becomes more favorable as the pH is lowered. The critical concentration for filament formation is also decreased at lower pH. The kinetic data do not support fragmentation occurring under any of the conditions examined. Furthermore, as Mg^{2+} exchange for Ca^{2+} at a high-affinity site ($K_d < 10^{-9}$ M) fails to alter significantly the polymerization kinetics, Ca^{2+} release from this site appears unnecessary for either the nucleation or the elongation of actin filaments.

Actin undergoes transformation from a monomeric species (G-actin) to a long helical polymer (F-actin)[1] by a process classically described by Oosawa and Kasai (1962) as a nucleation–elongation reaction. The kinetic mechanism by which actin polymerizes has been studied in extensive detail [e.g., see reviews by Korn (1982), Frieden (1985), and Pollard and Cooper (1986)]. Polymerization is known to be strongly influenced in vitro by environmental variables such as pH, temperature, and the species and concentration of cation present (Kasai et al., 1962; Kasai & Oosawa, 1968; Zimmerle & Frieden, 1986). As such factors are undoubtedly important in vivo as well, an understanding of the cellular activity of actin may first require detailed knowledge of the influence of these factors.

Different kinetic mechanisms have been proposed for the effect of Mg^{2+} binding and subsequent conformational changes on actin nucleation and filament elongation. While actin isomerization has been suggested by both Frieden (1983) and Keiser et al. (1986) to be a rate-limiting step in the Mg^{2+}-induced polymerization of actin, Estes et al. (1987) recently proposed a mechanism in which the limiting step for actin nucleation is slow Ca^{2+} release. Complicating both data analysis and the comparison of results is the presence of multiple metal binding sites on G-actin. It is generally agreed that there is one site of high affinity. Only recently, however, has the Ca^{2+} affinity of the high-affinity site been measured and the remaining metal binding sites characterized into two distinct groups of low and moderate metal affinity (Gersham et al., 1986; Carlier et al., 1986; Zimmerle et al., 1987). Low-affinity metal binding sites appear to be nonspecific and important for filament elongation to proceed (Carlier et al., 1986; Martonosi et al., 1964). At least one of the three moderate-affinity divalent cation binding sites appears to induce a conformational change in actin which alters the rates of actin nucleation (Zimmerle et al., 1987). Finally, the occupancy of the binding site with high Ca^{2+} affinity is related to nucleotide exchange (Frieden & Patane, 1988; Selden et al., 1987).

Although it is known that the rate of actin polymerization increases rapidly at lower pH values (Oosawa & Kasai, 1971), a detailed examination of polymerization kinetics as a function of pH has never been reported. In the present paper, we examine the alteration of actin polymerization kinetics with pH. By fitting the experimental data to computer simulations generated by numerical integration of rate equations, we test two proposed mechanisms for actin polymerization. We conclude the mechanism originally proposed by Frieden (1983) appears valid between pH 6 and 8 and that proton binding induces a conformational change and a large increase in the stability of actin dimers which, in turn, is responsible for the faster polymerization observed at lower pH.

Materials and Methods

Chemicals. BAPTA and *N*-(1-pyrenyl)iodoacetamide were purchased from Molecular Probes. ATP (disodium salt) and EGTA were purchased from Sigma, and all other reagents were analytical grade.

Protein Purification and Modification. Preparation and storage of rabbit muscle G-actin were as described in the preceding paper (Zimmerle & Frieden, 1988). Actin labeled with *N*-(1-pyrenyl)iodoacetamide (pyrene-actin) was prepared by a modification (Tellam & Frieden, 1982) of the method of Kouyama and Mihashi (1980). The molar ratio of dye/actin was between 0.8 and 0.99.

Data Analysis. Analyses of the data to the kinetic mechanisms described in this paper were performed by using the programs KINSIM (version 3.41) and FITSIM as described in the preceding paper (Zimmerle & Frieden, 1988). These pro-

† This work was supported in part by Grant DK 13332 from the National Institutes of Health.
* Address correspondence to this author at Box 8094, Washington University School of Medicine, 660 S. Euclid, St. Louis, MO 63110.
‡ Present address: Miles Inc., P.O. Box 70, Elkhart, IN 46515.

[1] Abbreviations: Ca–G-actin, monomeric actin with bound Ca^{2+}; Mg–G-actin, monomeric actin with bound Mg^{2+}; F-actin, polymerzied filamentous actin; pyrene-actin, actin labeled with *N*-(1-pyrenyl)iodoacetamide; Tris, tris(hydroxymethyl)aminomethane; EDTA, ethylenediaminetetraacetic acid; NBD, 7-chloro-4-nitro-2,1,3-benzoxadiazole; C_c, critical concentration; AEDANS-actin, actin labeled with *N*-(iodoacetyl)-*N'*-(5-sulfo-1-naphthyl)ethylenediamine; SSQ, sum of squares.

0006-2960/88/0427-7766$01.50/0

grams, which have been described previously (Barshop et al., 1983; Zimmerle et al., 1987), allow experimental data to be fit to simulations of kinetic rate equations.

Analyses of the data at each pH were generally performed by using five to six full time courses of G-actin polymerization initiated by the addition of Mg^{2+}. The polymerization time courses routinely used included ones 5–7-fold different in actin concentration with Mg^{2+} and Ca^{2+} concentrations held constant, ones where the Mg^{2+} concentrations were at least 4-fold different with actin and Ca^{2+} concentrations held constant, and ones where the Ca^{2+} concentrations were at least 20-fold different. These set of conditions were found to be adequate to obtain statistically significant fits to the data. Other time courses with intermediate conditions, while generally not included in the regression analysis due to computer time restraints, were also found to fit the experimental data using the parameters obtained by the regression analysis using the more extreme conditions. Polymerization at a given experimental condition was repeated on different days to ensure time courses obtained were reproducible.

Fits to the experimental data were considered adequate when the residuals between the predicted and experimental data for all reactions tested were relatively small and convergence had occurred. Standard errors in the final kinetic parameters were generally less than 20%, and R^2 values were all above 0.98. The weighted mean SSQ was used in comparing fits to experimental data at a given pH.

Determinations of the equilibrium concentrations for free metal cations in the presence of ATP at each pH were calculated by using a program described by Storrer and Cornish-Bowden (1979) using the following dissociation constants: $MgATP^{2-}$, 5 μM; $CaATP^{2-}$, 5 μM; $MgHATP^{1-}$, 1.7 mM; $CaHATP^{1-}$, 3.3 mM; $HATP^{3-}$, 0.11 μM (Frieden & Patane, 1988; Phillips et al., 1966).

Polymerization Studies. Actin polymerization was monitored by using the fluorescence change of a trace amount of pyrene-labeled (generally <1%) actin as described elsewhere (Tellam & Frieden, 1982). Fluorescence measurements were obtained by using a Spex fluorometer in a mode which corrects for signal fluctuations as a result of light intensity changes. To measure pyrene-actin fluorescence, excitation and emission wavelengths of 365 and 386 nm, respectively, were used. Data were collected continuously on a PDP 11/23 and stored in digital mode on a MicroVAX II for later analysis. For polymerization reactions using Mg–G-actin, 250 μM Mg^{2+} and either 100 μM EGTA (pH 8.0) or 100 μM BAPTA (pH 6.0) were added 5 min before the initialization of polymerization. Previous experiments have confirmed these conditions are sufficient to remove Ca^{2+} at the high-affinity site (Zimmerle et al., 1987).

RESULTS

Effect of pH on Actin Polymerization. Any general mechanistic description of actin polymerization is dependent on two processes, the rate of nucleation and the stability of filament formed. Figure 1 shows, at 20 °C and as a function of pH, the Mg^{2+}-induced polymerization of 10 μM G-actin in G buffer (200 μM Ca^{2+} and 200 μM ATP). Two effects of lowering the pH are immediately apparent; the lag phase becomes smaller, and the rate of polymerization becomes faster. Thus, the half-time for polymerization decreases from 18 to 2 min as the pH is lowered from pH 8 to 6, and the lag period, calculated here as a tangent drawn through the point of fastest polymerization, decreases from approximately 240 to 30 s. Polymerization reactions below pH 6 are not described here since the final extent, as measured by pyrene fluorescence,

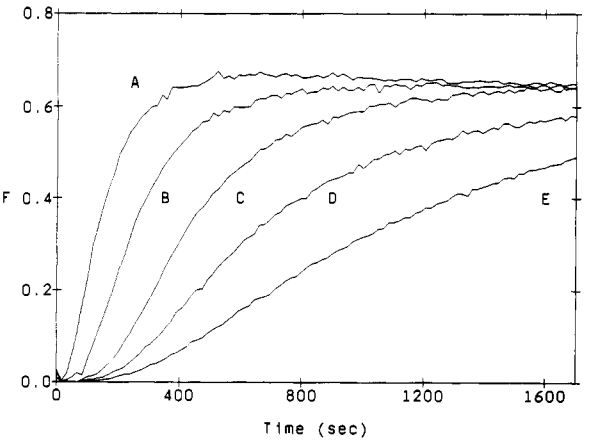

FIGURE 1: Effect of pH on actin polymerization at 20 °C. The lines show the fluorescence increase associated with the polymerization of 10 μM G-actin, 1% of which was pyrene labeled, induced by the addition of 1.8 mM Mg^{2+} in 200 μM ATP and 200 μM Ca, in a buffer of the appropriate pH at 20 °C. From left to right are polymerizations at pH 6.0 (A), 6.5 (B), 7.0 (C), 7.5 (D), and 8.0 (E). The time courses at each pH have been normalized to the same final fluorescence value.

becomes significantly less. At the present time, it is not known whether this decrease is due to actin denaturation at low pH or some other process.

Metal Binding at Low-Affinity Sites of Actin. Carlier et al. (1986) recently reported that the rate of filament elongation is similar regardless of whether Ca^{2+} or Mg^{2+} is bound at the low-affinity metal binding sites. They proposed the large rate difference between Ca^{2+}-induced and Mg^{2+}-induced polymerization is a consequence of differences induced by the metal species bound at the high-affinity site, while the metal species bound at the low-affinity site makes little difference. This is consistent with the view that metal binding to the low-affinity sites is nonspecific and conformational changes resulting from metal binding to these sites are a general salt-induced effect (Zimmerle & Frieden, 1988; Carlier et al., 1986).

We confirmed the results of Carlier et al. (1986) in the following manner. Actin was first incubated at pH 6 for 5 min under conditions to bring about the Mg^{2+}-dependent conformational change and to remove most of the actin-bound Ca^{2+} (300 μM Mg^{2+} and 50 μM BAPTA). This actin is referred to here as Mg–G-actin. It was then induced to polymerize by the subsequent addition of either 1.7 mM Mg^{2+} or 1.7 mM Ca^{2+}. Figure 2 shows the preincubation with Mg^{2+} and BAPTA markedly decreased the lag phase associated with G-actin containing bound Ca^{2+} (Frieden, 1982; Gershman et al., 1984) and that the subsequent polymerization induced by Ca^{2+} or Mg^{2+} addition is nearly identical regardless of the metal species added.

A pH of 6 was chosen for this experiment since, in comparison to pHs above this, polymerization is relatively fast in comparison to either the rate of Mg^{2+}–Ca^{2+} exchange at the high-affinity site or the rate of actin isomerization. Therefore, polymerization induced by metal binding at the low-affinity sites can occur before the replacement of Mg^{2+} at either the high- or the moderate-affinity site by Ca^{2+}. At pH 8, Mg–G-actin initially shows similar elongation rates upon the addition of either Ca^{2+} or Mg^{2+}, but at later times, the polymerization rate in the presence of Ca^{2+} becomes significantly slower (data not shown).

Effect of Mg^{2+} Preincubation at Low pH. Since the preincubation of G-actin with Mg^{2+} at pH 6 removes most of the initial lag phase, a result also seen at pH 8 (Zimmerle & Frieden, 1986; Gersham et al., 1984; Frieden, 1983), the replacement of Ca^{2+} by Mg^{2+} appears to be a rate-limiting step

in the Mg^{2+}-induced polymerization of actin throughout the pH range examined. However, it is unclear whether cation exchange at the moderate-affinity site or at the high-affinity site is responsible for this lag period (Zimmerle et al., 1987; Carlier et al., 1986; Estes et al., 1987). The fact that changes in the fluorescence of AEDANS-actin are related to metal exchange at the moderate-affinity site does not eliminate the possibility that metal exchange at the high-affinity site may also alter nucleation rates. Therefore, we attempted to distinguish, on the basis of fitting actin polymerization data to computer-generated simulations of each kinetic mechanism, between the two possibilities.

One kinetic mechanism, described by Scheme I, assumes Mg^{2+} binding to a site of moderate metal affinity and Mg^{2+} binding to a site of low affinity are prerequisites for the Mg^{2+}-induced polymerization of actin. This mechanism is essentially identical with one proposed previously by Frieden (1983). The other kinetic mechanism, described later by Scheme II, assumes that slow Ca^{2+} release is necessary for nucleation to occur but filament elongation is dependent only upon the binding of metal to low-affinity sites. In contrast to Scheme I, the elongation rate is similar regardless of the metal species bound at the high-affinity site. This latter mechanism includes the initial polymerization steps recently proposed by Estes et al. (1987). Thus, although each mechanism assumes Ca^{2+}–Mg^{2+} exchange is responsible for the initial lag phase found in the Mg^{2+}-induced polymerization of G-actin, they differ in the description of the kinetic steps for this lag. We will discuss the fits obtained with the scheme incorporating a Mg^{2+}-induced conformational change first.

Fits of Actin Polymerization to Scheme I. The mechanism previously found to fit the Mg^{2+}-induced actin polymerization data at pH 8 between 10 and 35 °C (Frieden, 1983; Zimmerle & Frieden, 1986), slightly modified, is shown in Scheme I. The first two steps in Scheme I incorporate the Mg^{2+}-induced actin isomerization, as detected by using actin labeled with AEDANS, while step 7 describes filament elongation.

Scheme I

$$A + Ca \underset{}{\overset{K_{Ca}}{\rightleftharpoons}} ACa \quad (1)$$

$$A + Mg \overset{K_{Mg}}{\rightleftharpoons} AMg \underset{k_{-iso}}{\overset{k_{+iso}}{\rightleftharpoons}} A'Mg \quad (2)$$

$$A'Mg + M \overset{K_M}{\rightleftharpoons} A'MgM \quad (3)$$

$$2A'MgM \overset{K_{dimer}}{\rightleftharpoons} \{A'MgM\}_2 \quad (4)$$

$$A'MgM + \{A'MgM\}_2 \overset{K_{trimer}}{\rightleftharpoons} \{A'MgM\}_3 \quad (5)$$

$$A'MgM + \{A'MgM\}_3 \overset{K_{tetra}}{\rightleftharpoons} \{A'MgM\}_4 \quad (6)$$

$$\vdots$$

$$A'MgM + \{A'MgM\}_n \underset{k_{-e}}{\overset{k_{+e}}{\rightleftharpoons}} \{A'MgM\}_n \quad (7)$$

In Scheme I, A is monomeric G-actin containing metal bound at the high-affinity site, ACa or AMg is G-actin containing either bound Ca^{2+} or Mg^{2+} at the moderate-affinity site(s), and A'Mg (Mg^{2+}-activated actin) is the Mg^{2+}-induced actin monomer. K_{Mg} describes the initial binding of Mg^{2+}. K_M describes metal binding at the low-affinity cation binding sites on actin. However, since in the experiments presented here, Mg^{2+} is generally the only metal at high enough concentration to be bound at these sites, K_M represents the Mg^{2+} affinity of these sites. The rate constants k_{+e} and k_{-e} in Scheme I describe the overall elongation and disassembly rates respectively, of the F-actin filament.

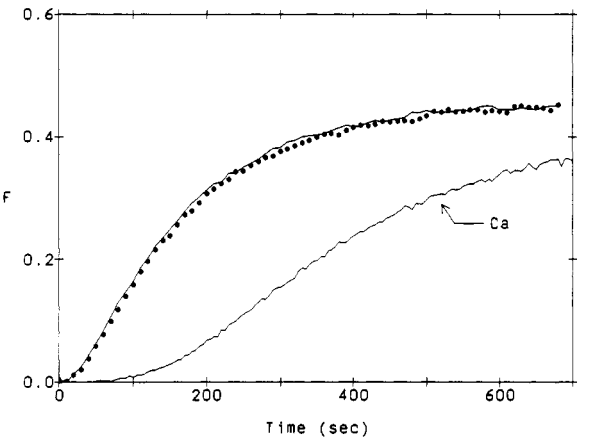

FIGURE 2: Effect of Ca^{2+} or Mg^{2+} addition to 3 μM G-actin at pH 6 and 20 °C. G-Actin was preincubated for 5 min against 30 μM BAPTA and 300 μM Mg in 2 mM MES buffer containing 200 μM ATP. At time zero, either 1.7 mM Ca (solid line) or 1.7 mM Mg (closed circles) was added. A control is also shown (solid line labeled Ca) where 2 mM Mg^{2+} is added to 3 μM G-actin in the presence of 1 μM free Ca^{2+} and 2 mM MES buffer, pH 6.

Table I: Fits of Polymerization Data to Scheme I

	pH of polymerization				
constant	6.0	6.5	7.0	7.5	8.0[a]
K_{Mg} (μM)	230	280	140	1200	1100
k_{+1} (μM^{-1} s^{-1})	0.011	0.012	0.081	0.113	0.14
k_{-1} (s^{-1})	0.002	0.002	0.017	0.0045	0.01
K_M[b] (μM)	450	1400	5800	2300	2300
K_{Ca} (μM)	140	290	6	32	15
K_{dimer} (μM)	9.6×10^3	5.2×10^3	1.8×10^4	1.9×10^6	3.0×10^6
K_{trimer} (μM)	4	5	0.400	1.7	2
K_{tetra} (μM)	0.6	20	18	0.18	0.15
k_{-e}/k_{+e}[c] (μM)	0.069	0.012	0.02	0.18	0.15
weighted mean SSQ	6×10^{-5}	3×10^{-4}	4×10^{-4}	1×10^{-4}	ND[d]

[a] Taken from Zimmerle and Frieden (1986). [b] Binding values are for Mg^{2+} binding. [c] k_{+e} is assumed to be equal to 1 μM^{-1} s^{-1}. [d] Not determined.

We assumed an elongation rate of 1 μM^{-1} s^{-1} for the fits obtained here, consistent with previous values in the literature and within the range assumed for a diffusion-controlled process (Lal et al., 1984; Pollard, 1986). If this assumed value for the elongation rate is underestimated, the rate constant for dimer formation will be overestimated by the same amount (Zimmerle & Frieden, 1986), but the quality of the final fits obtained as well as the conclusions reached will remain the same.

Table I is a summary of the kinetic constants found to best describe the Mg^{2+}-induced polymerization using Scheme I at each pH examined. Figure 3 shows a representative fit of the simulations to experimental polymerization data obtained at pH 6. The quality of fits obtained at higher pH values is similar. On lowering the pH, the following trends occur: The forward rate constant for the isomerization of actin induced by Mg^{2+} binding is reduced 10-fold, although the overall Mg^{2+} affinity ($K_{Mg}k_{-1}/k_1$) shows no trend and varies only 2-fold. The formation of dimer becomes approximately 2.5 orders of magnitude more favorable on going from pH 8 to 6, while little change occurs in trimer formation over this pH range.

Although fits to either kinetic scheme show K_M is lower at pH 6 compared to pH 8, the apparent tighter binding of Mg^{2+} at the low-affinity site is most likely an artifact caused by the protonation of actin at low pH. On the basis of studies using

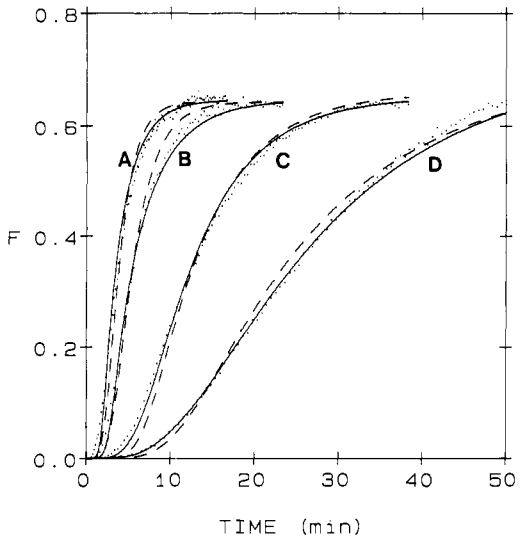

FIGURE 3: Fits of the experimental data to two different kinetic mechanisms. Fits to the data using Scheme I are represented by the solid line while fits to the data using Scheme II are represented by the dashed line. The experimental polymerization conditions shown contained 200 μM Ca in 2 mM MES buffer at pH 6 at 20 °C along with (A) 5 μM G-actin and 2 mM Mg, (B) 5 μM G-actin and 1 mM Mg, (C) 2 μM G-actin and 2 mM Mg, and (D) 1 μM G-actin and 2 mM Mg.

Scheme II

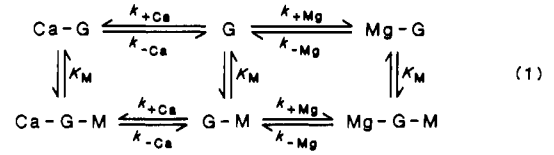

(1)

$$Mg\text{-}G\text{-}M + Mg\text{-}G\text{-}M \underset{}{\overset{K_{dimer}}{\rightleftharpoons}} (Mg\text{-}G\text{-}M)_2 \quad (2)$$

$$Mg\text{-}G\text{-}M + (Mg\text{-}G\text{-}M)_2 \overset{K_{trimer}}{\rightleftharpoons} (Mg\text{-}G\text{-}M)_3 \quad (3)$$

$$Mg\text{-}G\text{-}M + (Mg\text{-}G\text{-}M)_3 \overset{K_{tetra}}{\rightleftharpoons} (Mg\text{-}G\text{-}M)_4 \quad (4)$$

$$M\text{-}G\text{-}M + (Mg\text{-}G\text{-}M)_n \underset{k_{-e}}{\overset{k_{+e}}{\rightleftharpoons}} (Mg\text{-}G\text{-}M)_n \quad (5)$$

AEDANS-actin (Zimmerle & Frieden, 1988), protonation of actin or metal binding to the low-affinity sites result in similar, if not identical, effects. Thus, increasing the H^+ concentration is effectively the same as increasing the Mg^{2+} concentration. Furthermore, since metal binding to actin is inhibited by proton binding (Martonosi et al., 1964), the Mg^{2+} affinity at the low-affinity site may be less than that indicated by computer fitting of the polymerization data to either Scheme I or Scheme II.

Fits of Actin Polymerization to Scheme II. The mechanism described by Scheme II includes the initial polymerization steps recently proposed by Estes et al. (1987). In this mechanism, any monomeric actin species with cation bound at the low-affinity site is allowed to elongate (Scheme II, step 5), but only actin with Mg^{2+} bound at the high-affinity site can nucleate (Scheme II, steps 2–4). Although it is known that actin with a tightly bound Ca^{2+} can polymerize, albeit slowly under the conditions in which polymerization is carried out here, nucleation induced by Ca^{2+} can safely be ignored.

Step 1 of Scheme II shows complex equilibria in which metals compete for two distinct sites on G-actin monomer, the metal-free form of which is represented by the symbol G. It is assumed in step 1 that no interactions occur between the low-affinity and high-affinity sites on the actin molecule. Metal binding at the low-affinity site does not alter the rate constants associated with metal binding at the high-affinity site. Species to the left of the G symbol represent metal binding to the site with high affinity for Ca^{2+}. Species to the right side of G represent metal binding to the low-affinity site. M represents either Ca^{2+} or Mg^{2+}.

Table II: Fits of Polymerization Data to Scheme II

	pH of polymerization				
constant	6.0	6.5	7.0	7.5	8.0[a]
k_{-Ca}[b] (s^{-1})	0.009	0.06	0.03	0.18	0.14
k_{+Mg} (μM^{-1} s^{-1})	0.083	0.06	0.13	0.018	0.08
k_{-Mg} (s^{-1})	0.004	0.005	0.03	0.013	0.01
K_M[c] (μM)	460	1000	4000	2200	1500
K_{dimer} (μM)	8.5×10^4	1.4×10^6	8.7×10^4	2.4×10^6	4.4×10^6
K_{trimer} (μM)	0.005	0.001	0.001	0.12	0.15
k_{-e}/k_{+e} (μM)	0.005	0.02	0.07	0.12	0.15
weighted mean SSQ	2×10^{-4}	4×10^{-4}	7×10^{-4}	2×10^{-4}	ND[d]

[a] Based on data of Zimmerle and Frieden (1986). [b] k_{+Ca} is assumed equal to 1 μM^{-1} s^{-1}. [c] Values given are for Mg^{2+}. [d] Not determined.

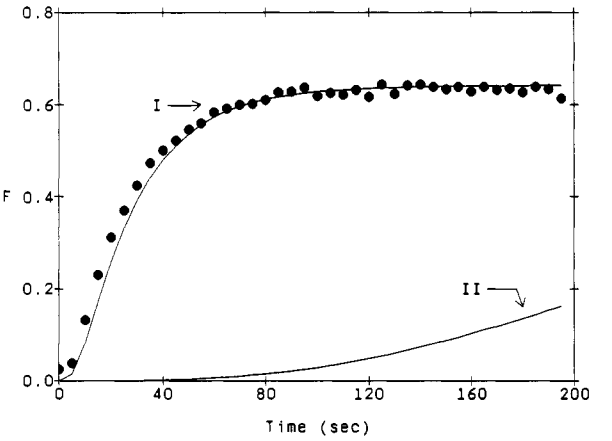

FIGURE 4: Comparison of the predicted polymerization curves using Scheme I and Scheme II for Mg^{2+}-activated actin at pH 6 and 20 °C. Mg^{2+}-activated actin was formed at pH 8 by the addition of 200 μM Mg^{2+} to a solution containing 10 μM actin, 200 μM ATP, 50 μM Mg^{2+}, and 1 mM Tris. Polymerization was initiated by an amount of 1 M MES sufficient to lower the pH to 6. The closed circles represent the actual data while the solid line through the points, labeled I, represents the predicted polymerization curve using Scheme I and the kinetic constants for this scheme shown in Table I. The lower solid line labeled II represents the predicted polymerization curve using Scheme II and the kinetic constants shown for this scheme in Table II.

Table II presents a summary of the kinetic constants found best to describe the data by simulations utilizing Scheme II. Dimer formation becomes about 50-fold more favorable from pH 8 to 6 while both trimer formation and filament elongation also generally become more favorable on lowering the pH. A representative fit of the simulations to the experimental polymerization data is shown by Figure 3.

As demonstrated by Carlier et al. (1986) and in the present paper, Ca^{2+} bound at the low-affinity site appears to promote actin polymerization in a manner similar to when Mg^{2+} binds at this site. However, in the polymerizations reported here, Ca^{2+} concentrations are sufficiently low such that little or no Ca^{2+} will be bound at the low-affinity sites on actin.

Polymerization/Depolymerization Induced by pH Changes. Figures 4 and 5 show that the polymerization or depolymerization of actin can be induced by pH changes. Figure 4 shows rapid polymerization of Mg^{2+}-activated actin takes place upon lowering the pH from 8 to 6. Mg^{2+}-activated actin, or actin having undergone the Mg^{2+}-induced isomerization, was pre-

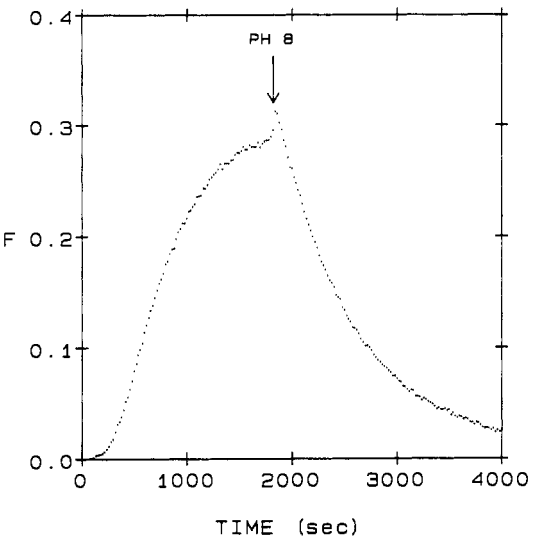

FIGURE 5: Depolymerization of F-actin induced by an increase in pH. At zero time, 550 μM Mg is added to 2.3 μM actin, 5% of which is pyrene labeled, in 500 μM ATP, ATP, and 2 mM MES buffer, pH 6 at 20 °C. At the arrow marked pH 8, the pH was rapidly increased by the addition of a 1 M solution of Tris sufficient to raise the pH to 8.3. The cuvette was inverted twice to thoroughly mix the solution.

pared at pH 8 by a 5-min preincubation of actin with 200 μM Mg^{2+} and 200 μM ATP (Zimmerle et al., 1987). The polymerization of Mg^{2+}-activated actin at pH 6 is consistent with our findings that at least some polymerization of actin occurred upon the dialysis of G-actin at pH 6 versus Mg^{2+} concentrations as low as 50 μM.

Since very low actin concentrations polymerize readily at low pH, and polymerization can apparently be induced simply by lowering the pH (Figure 4), we tested whether actin depolymerization could be brought about by raising the pH. Figure 5 shows that nearly complete depolymerization of F-actin in the presence of 550 μM Mg^{2+}, 500 μM ATP, and 1 μM Ca^{2+} occurs when the pH is rapidly raised from pH 6 to pH 8.2 by the addition of 1 M Tris. Thus, the overall critical concentration changes substantially between pH 6 and 8 under these conditions.

Distinguishing between Scheme I and Scheme II. Figure 3 shows that the differences in the fits to Scheme I and those to Scheme II at pH 6 were minimal with G-actin in the presence of Ca^{2+} (Ca–G-actin). However, as indicated by Frieden and Goddette (1983), it is important to obtain data over the widest possible range of experimental conditions when distinguishing between kinetic schemes. Therefore, other experimental conditions were explored which could distinguish between the two schemes.

Through simulations using KINSIM, we determined that the expected polymerization characteristics of actin containing bound Ca^{2+} at the high-affinity site and bound Mg^{2+} at the moderate-affinity site are different between Scheme I and Scheme II. Scheme I predicts little or no lag phase in the polymerization in contrast to the simulations using Scheme II. As the predicted difference between simulations using Scheme I and Scheme II was largest when Ca^{2+} release from the high-affinity site was slowest, a pH of 6 was chosen for the following experiment.

Mg^{2+}-activated actin was formed by preincubation of actin with 250 μM Mg^{2+} for 5 min in the presence of 1 μM Ca^{2+} at pH 8. This condition induces actin isomerization by Mg^{2+}, but at least 70% of the actin retains Ca^{2+} at the high-affinity site (Zimmerle et al., 1987). As Figure 4 shows, when the pH is rapidly lowered to 6, actin polymerization is induced immediately with almost no lag phase. These experimental data fit well to those predicted by Scheme I (upper curve, Figure 4) but very poorly to those predicted by Scheme II (lower curve, Figure 4). Attempts to simultaneously fit data obtained using Mg^{2+}-activated actin and Ca–G-actin and Scheme II yielded an overall poorer fit. This is to be expected for nonlinear regression fitting of the data if Scheme II cannot be used to explain the polymerization of Mg^{2+}-activated actin (Zimmerle and Frieden, unpublished experiments).

Discussion

For any mechanistic description of actin polymerization, at least two events must be described: the extent of nucleation and the actin concentration at which net filament elongation occurs (i.e., the critical concentration, C_c). On the basis of nonlinear regression fitting of polymerization time courses obtained using pyrene-labeled actin, we conclude here that the C_c of F-actin and the nucleation of G-actin in the presence of Mg^{2+} become more favored as the pH is lowered from 8 to 6. This is in agreement with previous results (Kasai et al., 1962; Wang et al., 1988). Furthermore, we find that the mechanism best able to describe actin polymerization over the pH range from 6 to 8 is one which includes a Mg^{2+}-induced conformational change (Frieden, 1983).

Previously, Frieden and co-workers (Frieden & Goddette, 1983; Frieden, 1983) demonstrated individual rate constants can be obtained by the fitting of computer-generated simulations to experimental data. Recently, we used least-squares regression fitting of kinetic simulations to experimental data in distinguishing between rival kinetic mechanisms for a metal-induced actin isomerization (Zimmerle et al., 1987). Using this approach, we critically evaluated two proposed mechanisms of actin polymerization as a function of pH. One mechanism assumes a Mg^{2+}-induced isomerization is necessary for actin nucleation and elongation, as described by Frieden (1983), while the other mechanism assumes release of a tightly bound Ca^{2+} is necessary for actin nucleation. In reality, both mechanisms are necessarily simplistic as they ignore the fact that addition of Ca^{2+}, or for that matter any salt, can induce polymerization. Thus, Mg^{2+} binding to actin undoubtedly only alters the favorability of the nucleation and elongation steps and is not absolutely required for it. Under the experimental conditions presented here, however, nucleation and elongation should be regulated by Mg^{2+} binding.

Filament fragmentation does not appear to be an important component in the pH dependence of actin polymerization. Fragmentation can be included in either scheme by adding the step:

$$\{A'(Mg)_2\}_n \underset{k_a}{\overset{k_f}{\rightleftharpoons}} \{A'(Mg)_2\}_{2n}$$

where k_f is the rate of fragmentation, k_a the rate of reannealing, and $\{A'(Mg)_2\}_n$ the actin polymer. However, since no significant improvements in the fit were achieved by adding this term, it can be assumed filament fragmentation does not play a major role at least in the in vitro polymerization of actin under these conditions. This could be due either to the absence of fragmentation or to a rapid reannealing process.

Interestingly, the general trends found in the rate constants on going from pH 8 to 6 are similar regardless of whether the data were fit to Scheme I or Scheme II. Fitting the data to either mechanism indicates an increase in the extent of actin dimer formation of 2 orders of magnitude on going from pH 8 to 6. The ratio between Ca^{2+}/Mg^{2+} binding at the moderate- (Scheme I) or the high- (Scheme II) affinity sites, a limiting step for nucleation in either scheme, remains nearly identical

at 5-fold. The value for K_M shows a maximum value at pH 7, with the value at pH 6 3–5-fold less than the value at pH 8. The major difference between the fits using Scheme I and Scheme II is whether trimer and tetramer formation is less favorable than the monomer–filament dissociation constant (k_{-e}/k_{+e}).

Scheme I is chosen over Scheme II since the presence of a significant lag phase with Mg^{2+}-activated actin at pH 6 by the latter scheme is not present (Figure 4). Attempts to fit the data to a modified Scheme II where slow Ca^{2+} release is needed before filament elongation failed. The very slow Ca^{2+} release rates found at low pH are simply not consistent with the much faster rates of polymerization. The two mechanisms tested here are by no means the only possibilities for kinetically describing the polymerization of actin. In fact, Carlier et al. (1986) recently proposed a mechanism similar to Scheme I, but different in that the Mg^{2+}-induced conformational change is required only for actin nucleation and not for filament elongation. Although fits to the polymerization data at pH 7.5 using this mechanism were poorer, they were not significantly so. At this time, it is not possible to find experimental conditions which can distinguish between Scheme I and the mechanism proposed by Carlier et al. (1986).

At pH 8, the rate constants were obtained for the Mg^{2+}-induced conformational change using AEDANS-actin (Zimmerle & Frieden, 1986) are consistent with the rate constants obtained by fitting the full time course of actin polymerization, but unfortunately, these constants differ from those obtained by Carlier. The differences may be due to their use of EGTA (Zimmerle et al., 1987). A difference between the scheme favored by Carlier et al. (1986) and that of Scheme I is related to whether further actin isomerization occurs as polymerization proceeds. Unfortunately, although there is a further increase in the fluorescence of AEDANS-actin upon polymerization, as predicted by Scheme I, it is difficult to distinguish whether this increase is due to the shifting of the equilibrium toward the Mg^{2+}-activated conformer or to a conformational change upon polymerization (Zimmerle & Frieden, unpublished data). Thus, the strongest argument for Scheme I to date is the fact that slow Ca^{2+} release can occur independent of Mg^{2+} binding (Zimmerle et al., 1987).

Assuming, then, Scheme I to be a more accurate representation of the mechanism, it can be concluded the most sensitive step to pH changes is the extent of dimer formation. It is of interest that this is the same step we have previously shown to be extremely sensitive to temperature (Zimmerle & Frieden, 1986). This suggests that the pH and temperature dependence of dimer formation is related and the effect of temperature is due, at least in part, to that of a temperature-related shift in the pK_a for one or more ionizable residues.

The analysis of the Mg^{2+}-induced polymerization of actin as a function of pH presented here suggests the importance of one or more actin conformational changes prior to monomer–filament association. From kinetic measurements of actin filament elongation, Keiser et al. (1986) suggested that G-actin exists in both a slow and a rapid polymerizing conformation with the exchange between these forms possibly regulated by Mg^{2+} binding. Miki et al. (1987) suggested a similar hypothesis on the basis of phalloidin interaction with chemically modified actin. Finally, spectroscopic evidence of actin isomerization prior to polymerization was found by Merkler et al. (1987). This latter result is consistent with our own observations demonstrating spectroscopic changes concomitant with the isomerization of actin induced by Mg^{2+} binding (Zimmerle and Frieden, unpublished observation).

Indeed, conformational changes induced by the addition of metal cations have been detected by a variety of methods (Frieden et al., 1980; Merkler et al., 1987; Rich & Estes, 1976; Barden & dosRemedios, 1985; Zimmerle et al., 1987). Recent evidence collected by both Gershman et al. (1987) and Frieden and Patane (1988) suggests the nucleotide binding properties of G-actin are quite dependent upon whether Ca^{2+} or Mg^{2+} is bound to the actin. Since the stability of F-actin appears dependent upon ATP hydrolysis (Pantaloni et al., 1985), and nucleotide binding is altered by cation exchange, a mechanism by which Mg^{2+} binding alters polymerization kinetics is suggested (Carlier et al., 1986). This is supported by the data of Frieden and Patane (1985) which showed ADP–actin, in contrast to ATP–actin, does not undergo isomerization in response to Mg^{2+} addition. Thus, a wealth of evidence exists for metal-dependent actin conformations which alter the kinetics of polymerization.

A considerable amount of experimental evidence argues against the recent suggestion by Matsudaira et al. (1987) that actin polymerization occurs by a simple condensation mechanism. Certainly, the kinetic modeling of actin polymerization between pH 6 and 8 does not support this hypothesis. Indeed, the results of our kinetic modeling indicate that under the polymerization conditions reported by Matsudaira et al. (1987) it would be difficult to detect any significant lag phase, as well as to prevent the preformation of any nuclei. Thus, it is not surprising that no evidence for a nucleation step was detected by their experiments.

Errors in fitting the polymerization data could occur if changes in pyrene fluorescence do not directly measure the assembly of actin into filament. Although both Carlier et al. (1986) and Grazi and Lanzara (1987) have demonstrated the increase in the fluorescence of pyrenyl-labeled actin may not be directly correlated to the formation of F-actin, the differences with Mg^{2+}-induced polymerization are undoubtedly quite small. In fact, if the cause of the nonlinearity in pyrene fluorescence resides in the uncoupling of ATP hydrolysis from polymerization, the fluorescence will deviate the most from measuring the actual amount of F-actin under experimental conditions where high concentrations of Ca–actin are polymerized by Ca^{2+} (Carlier et al., 1986), conditions not analyzed here. Following polymerization using NBD-Cl-labeled actin is complicated by its fluorescence sensitivity to divalent metal exchange. As shown above, separation of this fluorescence change from changes induced by polymerization may not be straightforward. Thus, this probe does not appear to be any better probe than pyrene-actin for following actin polymerization.

In conclusion, we propose the polymerization of actin is more favored at lower pH largely due to the increased favorability of actin dimer formation and to the induction of the salt-induced conformation by protons (Zimmerle & Frieden, 1988). This appears particularly true for Mg^{2+}-activated actin. We also demonstrate that a previously proposed mechanism (Frieden, 1983) appears able to predict the polymerization of actin between the pH range of 6 and 8 and that full time course simulations are an important tool both in the determination of individual rate constants and also in distinguishing between kinetic mechanisms.

ACKNOWLEDGMENTS

We thank Kalliopi Patane for her excellent technical assistance.

REFERENCES

Barden, J. A., & dos Remedios, C. G. (1985) *Eur. J. Biochem. 146*, 5–8.

Barshop, B. A. Wrenn, R. F., & Frieden, C. (1983) *Anal. Biochem. 130*, 134–145.
Bradford, M. M. (1976) *Anal. Biochem. 72*, 248–254.
Carlier, M., Pantaloni, D., & Korn, E. D. (1986) *J. Biol. Chem. 261*, 10778–10784.
Dawson, R. M. C., Elliott, D. C., Elliott, W. H., & Jones, K. M. (1986) *Data for Biochemical Research*, 3rd ed., Clarendon, Oxford.
Estes, J. E., Selden, L. A., & Gershman, L. C. (1987) *J. Biol. Chem. 262*, 4952–4957.
Frieden, C. (1982) *J. Biol. Chem. 257*, 2882–2886.
Frieden, C. (1983) *Proc. Natl. Acad. Sci. U.S.A. 70*, 2687–2691.
Frieden, C. (1985) *Annu. Rev. Biophys. Chem. 14*, 189–210.
Frieden, C., & Goddette, D. W. (1983) *Biochemistry 22*, 5836–5842.
Frieden, C., & Patane, K. (1985) *Biochemistry 24*, 4192–4196.
Frieden, C., & Patane, K. (1988) *Biochemistry 27*, 3812–3820.
Frieden, C., Lieberman, D., & Gilbert, H. R. (1980) *J. Biol. Chem. 255*, 8991–8993.
Gershman, L. C., Newman, J., Selden, L. A., & Estes, J. E. (1984) *Biochemistry 23*, 2199–2203.
Gershman, L. C., Selden, L. A., & Estes, J. E. (1986) *Biochem. Biophys. Res. Commun. 135*, 607–614.
Grazi, E., & Lanzara, V. (1987) *Arch. Biochem. Biophys. 257*, 115–122.
Houk, T. W., Jr., & Ue, K. (1974) *Anal. Biochem. 57*, 453–459.
Kasai, M., & Oosawa, F. (1968) *Biochim. Biophys. Acta 154*, 520–528.
Kasai, M., Asakura, S., & Oosawa, F. (1962) *Biochim. Biophys. Acta 57*, 13–21.
Keiser, T., Schiller, A., & Wegner, A. (1986) *Biochemistry 25*, 4899–4906.
Korn, E. D. (1982) *Physiol. Rev. 62*, 672–737.
Kouyama, T., & Mihashi, K. (1980) *Eur. J. Biochem. 114*, 33–38.
Lal, A. A., Brenner, S. L., & Korn, E. D. (1984) *J. Biol. Chem. 259*, 1441–1446.
Martonosi, A. Molino, C. M., & Gergely, J. (1964) *J. Biol. Chem. 239*, 1057–1064.
Matsudaira, P., Bordas, J., & Koch, M. J. (1987) *Proc. Natl. Acad. Sci. U.S.A. 84*, 3151–3155.
Merkler, I., Stournaras, C., & Faulstich, H. (1987) *Biochem. Biophys. Res. Commun. 145*, 46–51.
Mihashi, K., Nakabayashi, H., Yoshimura, H., & Ohnuma, H. (1979) *J. Biochem. (Tokyo) 85*, 359–366.
Miki, M., Barden, J. A., dos Remedios, C. G., Phillips, L., & Hambly, B. (1987) *Eur. J. Biochem. 165*, 125–130.
Oosawa, F., & Kasai, M. (1962) *J. Mol. Biol. 4*, 10–21.
Oosawa, F., & Kasai, M. (1971) *Biol. Macromol. 5*, 261–322.
Pantaloni, D., Hill, T. L., Carlier, M., & Korn, E. D. (1985) *Proc. Natl. Acad. Sci. U.S.A. 82*, 7207–7211.
Phillips, R. C., Philip, G., & Rutman, R. J. (1966) *J. Am. Chem. Soc. 88*, 2631–2640.
Pollard, T. D., & Cooper, J. A. (1986) *Annu. Rev. Biochem. 55*, 987–1037.
Rich, S. A., & Estes, J. E. (1976) *J. Mol. Biol. 104*, 777–792.
Selden, L. A., Gershman, L. C., Kinosian, H. J., & Estes, J. E. (1987) *FEBS Lett. 217*, 89–93.
Spudich, J. A., & Watts, S. (1971) *J. Biol. Chem. 246*, 4866–4871.
Storrer, A. C., & Cornish-Bowden, A. (1976) *Biochem. J. 159*, 1–5.
Tellam, R., & Frieden, C. (1982) *Biochemistry 21*, 3207–3214.
Wang, F., Sampogna, R., & Ware, B. R. (1988) *Biophys. J. 53*, 572a.
Zimmerle, C. T., & Frieden, C. (1986) *Biochemistry 25*, 4899–4906.
Zimmerle, C. T., & Frieden, C. (1988) *Biochemistry* (preceding paper in this issue).
Zimmerle, C. T., Patane, K., & Frieden, C. (1987) *Biochemistry 26*, 6545–6552.